

Hunting for Planet Nine by its perturbations on the Main Asteroid Belt

Albin Jonsson

Lund Observatory
Lund University



2019-EXA156

Degree project of 15 higher education credits
June 2019

Supervisor: Daohai Li

Lund Observatory
Box 43
SE-221 00 Lund
Sweden

Abstract

In recent years, scientists have found unconfirmed evidence for a ninth planet in the solar system at a very wide orbit. The parameters for this planet are poorly constrained. Current estimates mostly come from the effect the planet has on trans-neptunian objects. Here we investigate an alternative scenario, that is whether this proposed planet can exert observable perturbation on Main Belt asteroids through a particular resonance, active when the precession period of the asteroid is close to the orbital period of Planet Nine. As the apsidal precession period of the Main Belt asteroid is mainly driven by Jupiter, we first derive the precession period under the disturbance of Jupiter. We find that for asteroids at ~ 3 AU, the resonant condition is fulfilled when Planet Nine has a semi-major axis of ~ 600 AU. With the asteroids' behaviour known we add a Planet Nine to the simulations at the semi-major axis of optimal resonance conditions with asteroids positioned around 3 AU and analyse the output orbital data. However, in simulations where we assign Planet Nine a mass of 1000 Earth masses, no resonances are observed. To increase the chance of capture into resonance we let Planet Nine migrate inward or outward, causing the resonance to sweep through the asteroids. The mass of the planet is also increased to the somewhat unreasonable values of a solar mass and a tenth of a solar mass. With these implausible parameters, we find that the resonance is possible and when in libration, the periapsis of the asteroid is locked to the position of Planet Nine. Further studies are needed to determine the possibility of resonance for a more reasonable planetary mass and how effectively the planet can capture asteroids into resonance. We note that the effect investigated here may be the only known mechanism able to constrain the instantaneous location of Planet Nine.

Populärvetenskaplig beskrivning

Sedan den mindre kontroversen där Pluto degraderades från planet till dvärgplanet så har samhället varit överens om solsystemets åtta planeter: Mercurius, Venus, Jorden, Mars, Jupiter, Saturnus, Uranus och Neptunus. Detta kan dock komma att ändras, då forskning föreslår existensen av en planet större än vår egen bortom alla kända planeter. I detta arbete undersöks en helt ny metod som kan hjälpa oss att hitta den svårfångade planeten en gång för alla. Den kan möjligen hittas, inte genom att titta lång ut i vårt solsystem, utan genom att undersöka våra små grannar i Stora Asteroidbältet.

Asteroider färdas i sina elliptiska banor runt solen men Jupiter och andra planeter ”rycker” i dem, så att deras omloppsbanor ändras lite för varje omlopp. På så sätt roterar sakta den elliptiska banan runt Solen, i ett system som kan liknas vid en klocka. Det snabbare omloppet av asteroiden kan liknas vid minutvisaren, och för varje varv förskjuts ellipsens riktning ett litet steg liknande timvisaren. På så sätt är det lätt att förstå att asteroidens omlopps bana roterar mycket långsammare än asteroidens omlopp i denna bana. Huvudtanken bakom detta arbete är att denna rotation av en asteroids omlopps bana tar lika lång tid som en nionde planet tar för att genomföra ett omlopp. Den svaga tyngdkraft från den nionde planeten som når asteroiden kan då ”låsa fast” vinkeln mellan asteroidens elliptiska bana och planetens position.

Med dagens teknologi är detta något som är möjligt att undersöka. Genom att simulera solsystemets dynamik under miljontals år undersöks de optimala förhållanden som ger upphov till att vinkeln mellan planeten och asteroiden ”låses fast”. Tidigare studier har undersökt hur denna planets ”ryck” påverkar himlakroppar bortom Neptunus, men detta arbete skiljer sig från de tidigare på en viktig punkt. Till skillnad ifrån tidigare arbeten kan den metod som här undersöks härleda den aktuella positionen hos planeten.

Visar sig denna metod framgångsrik kan den spela en avgörande roll i att fastställa den nästan mytiska nionde planetens existens och omlopps bana. En sådan upptäck skulle vara den största framgång inom planetologin sedan 1846 då Neptunus upptäcktes. Upptäckten skulle inte enbart kunna ge oss kunskap om solsystemets förflutna, utan vara en fortsättning på en utav vetenskapens längst pågående sökande med en sekellång historia.

Contents

1	Introduction	4
1.1	Planet Nine	4
1.2	The Three-body Problem	5
1.3	Resonances in the Main Asteroid Belt	6
1.4	Orbital Resonance	7
2	The Main Asteroid Belt with Jupiter as Perturber	10
2.1	Numerical simulations	10
2.2	Data Analysis & Plotting	11
2.3	Interpretation	11
3	Planet Nine Simulations	15
3.1	Parameters of Planet Nine	15
3.2	Simulations over one million years	16
3.3	Simulations over twenty million years	18
3.4	Resonance strength	18
3.5	Migrating Planet Nine	21
3.5.1	Solar-massed Planet Nine simulations	21
3.5.2	Simulations with one tenth solar-mass	24
4	Discussion & Conclusion	27
A	Supplementary figures	30

List of Figures

1.1	A sketch on the geometry of the investigated system, where the angle $\bar{\omega}_{ast} - \lambda_9$ is librating around a fixed value due to the asteroid being captured into orbital resonance.	7
2.1	The strength of the FFT carried out on the varying longitude of perihelion along with the eccentricity of the orbit.	12
2.2	The period of precession for asteroids in the span 2.5-3.5 AU. The asteroids are massless bodies orbiting the sun in a system perturbed only by Jupiter.	13
3.1	Time evolution of the critical angle for the asteroid in the 1 Myr simulation with a precession period closest to the orbital period of Planet Nine.	17
3.2	Time evolution of the critical angle for the asteroid in the 20 Myr simulation with a precession period closest to the orbital period of Planet Nine.	19
3.3	Time evolution for the eccentricity of the same asteroid as in figure 3.2 from the 20 Myr simulation.	20
3.4	Time evolution of the critical angle of an asteroid in P9AJER with a solar-mass Planet Nine as the planet migrates inwards.	22
3.5	Phase-space diagram of the critical angle and eccentricity for two asteroids, one in P9AJER (coloured circles) and one in circulation (red crosses). The data for the librating asteroid is from the same asteroid as in figure 3.4, and for this case the colour gradient of the data points correspond to the integration time of the specific values.	25
3.6	Time evolutions of the critical angles for the asteroids in a system containing a migrating Planet Nine, with one tenth of a solar mass, simulated for 50Myr.	26

A.1	Similarly to figure 2.2, the data points are precession periods for asteroids orbiting the sun perturbed by Jupiter, but the asteroids lie in the span 3.0-3.8 AU. For the outer asteroids, the orbits become highly unstable due to the proximity of Jupiter.	30
A.2	Time evolution of the critical angle of an asteroid in the same system as 3.4, except Planet Nine migrates outwards. In this case, we observe the critical angle librating around $\sim 90^\circ$ and the asteroid is trapped into P9AJER	31

Chapter 1

Introduction

1.1 Planet Nine

The question of a ninth planet beyond Neptune has grown more relevant since the paper by Trujillo and Sheppard (2014), where trans-Neptunian objects were seen to cluster around a common perihelion beyond simple observational bias. By simulating a ninth planet of above-Earth mass, the same clustering could be generated as in the observations. This yet-to-be-confirmed/disputed planet was estimated to have a semimajor axis of several hundred astronomical units, far beyond any known planets in our solar system.

The hypothesis of a ninth planet, hereby referred to as Planet Nine, has been suggested by several studies. As our observation technology has improved, we have been able to map the orbits of many objects lying beyond our furthest known planet: Neptune. Investigations of the orbits of these trans-Neptunian object have revealed around a dozen of them to have arguments of perihelion, the angle between the perihelion and the intersection of the orbit with the celestial plane, centered around zero degrees. The perturbing effect of Planet Nine was held responsible for this Trujillo and Sheppard (2014). Another study argues that the inclination distribution of the distant bodies can be attributed to a perturbing body of planetary mass Batygin et al. (2019).

Under the assumption that there exists a Planet Nine, it must lie within the parameter space constrained by the dynamics of our solar system. A too distant planet would be lost due to galactic tides, whilst a too close and massive planet would cause notable perturbation on the well-known orbits of the planets Batygin et al. (2019). The mass of Planet Nine is also further constrained by the fact that at ~ 13 Jupiter masses fusion would occur and Planet Nine would instead be a star, making the Solar System part of a binary. A review of Planet Nine estimates the semi-major axis of the planet to 400 - 800 AU Batygin et al. (2019). At such

a distance, intuition tells us that Planet Nine does not affect the dynamics of the inner Solar System. However, with this project, we will show that this may not be the case.

At several hundreds of AU, Planet Nine's orbital period would be of the order of 10^4 years. Such periods may coincide the apsidal precession of asteroids in the Main Asteroid Belt. If the precession and orbital period were very close, the asteroid may be captured into orbital resonance with Planet Nine, where the apsidal. Observations of the asteroid should then reveal the perturbations caused by a Planet Nine, and the results could be used to further constrain the parameters of the planet.

In this project, we will investigate whether or not the capture of a Main Belt asteroid into orbital resonance by Planet Nine could be possible. The investigation was carried out numerically, by several simulations of the solar system containing a Planet Nine with different parameters. Analysis of the asteroids' orbits then revealed if they were trapped into resonance. In order to set up the context of the investigation, we briefly need to review the basics of a N -body system.

1.2 The Three-body Problem

The motions of objects in the solar system are governed by the simple laws of Newtonian mechanics. For a system of two bodies, with masses m_1, m_2 separated by the distance r , the physics is very simple with the two bodies attracting each other with the force

$$F = G \cdot \frac{m_1 m_2}{r^2}. \quad (1.1)$$

The two bodies can then form stable orbits around their common centre of mass. Viewing one of the masses as stationary, Kepler's first law states that the other body then moves on a fixed elliptical orbit with the stationary mass in one of the focal points of the ellipse. The orbit can be described by six parameters called orbital elements. They are the semi-major axis, eccentricity, inclination of the orbit relative to a reference plane, argument of perihelion, longitude of ascending node and the mean anomaly. For an orbit of nonzero inclination i , the orbit will intersect the reference plane at two points. The angle between a reference direction of the system and the intersection point where the orbit passes from below to above the reference plane is the longitude of the ascending node Ω , and the angle between the ascending node and the perihelion of the orbit is the argument of perihelion ω . The longitude of perihelion $\bar{\omega}$ is the angle between the perihelion and reference direction, easily calculated as

$$\bar{\omega} = \Omega + \omega. \quad (1.2)$$

The mean anomaly M describes the angle between the perihelion of the orbit and the position of the orbiting object when the orbit is approximated to be circular. In a simple two-body system all orbital elements except the mean anomaly, which is a linear function of time, are fixed and unchanging.

However, if introducing another object to the system, the system becomes more complicated. Here we consider a system of two planets orbiting a common star, each on their own trajectory. Yet as both planets have mass, they affect each other with a perturbing force. As a result, the orbital elements for each planet are no longer constant. With this complexity, the system becomes difficult to describe.

An approach to calculate the complex orbits in a three-body system is via a numerical integration method. The simplest example is the Euler method. Broadly speaking, for a system described by a differential equation and with known initial parameters, the instantaneous rate of change of the system is calculated. For a small enough timestep, the rate of change at the initial parameters represents well the average rate of change for the entire timestep. Iteration of this process allows the simulation of systems described by differential equations. The many stepwise calculations of the integration method are best performed in dedicated computer programs, as was done in this project. While the Euler method is easily understood, it relies only on the first order Taylor expansion. As such, it may deviate greatly from the actual system between steps. In the software, a more complex and accurate model of the integration method of higher order than Euler was applied. In this project we use a second-order mixed-variable symplectic integration, a method useful for fast simulations of hierarchical systems. In later simulations, where another object approaches stellar mass, we apply the Bulirsch-Stoer method which can accurately handle non-hierarchical systems.

1.3 Resonances in the Main Asteroid Belt

The Asteroid Belt consists of a large number of objects distributed over varying semi-major axis. Due to the distribution of orbital elements of the asteroids, many asteroids enter resonant conditions with the larger planets of the solar system. Many of these resonances are mean-motion resonances between the asteroids and the planets, where the orbital periods of asteroids and planets have ratios of two small integers. In regions where the resonances occur, a weaker resonance with Planet Nine is unlikely to be detectable. In order to detect the weaker resonance, it must occur in a parameter space of the asteroid belt devoid of other, stronger resonances.

The majority of asteroids in the asteroid belt are distributed within a section of orbits with a semi-major axis of 2.2-3.2 AU Murray and Dermott (1999). At these distances, the asteroids are affected by mean motion resonances with the

inner rocky planets. For the larger lengths of semi-major axis, resonances with Jupiter are more frequent. Due to the large mass of Jupiter in comparison to the rocky planets, the strength of Jupiter resonances are larger by orders of magnitude Gallardo (2006).

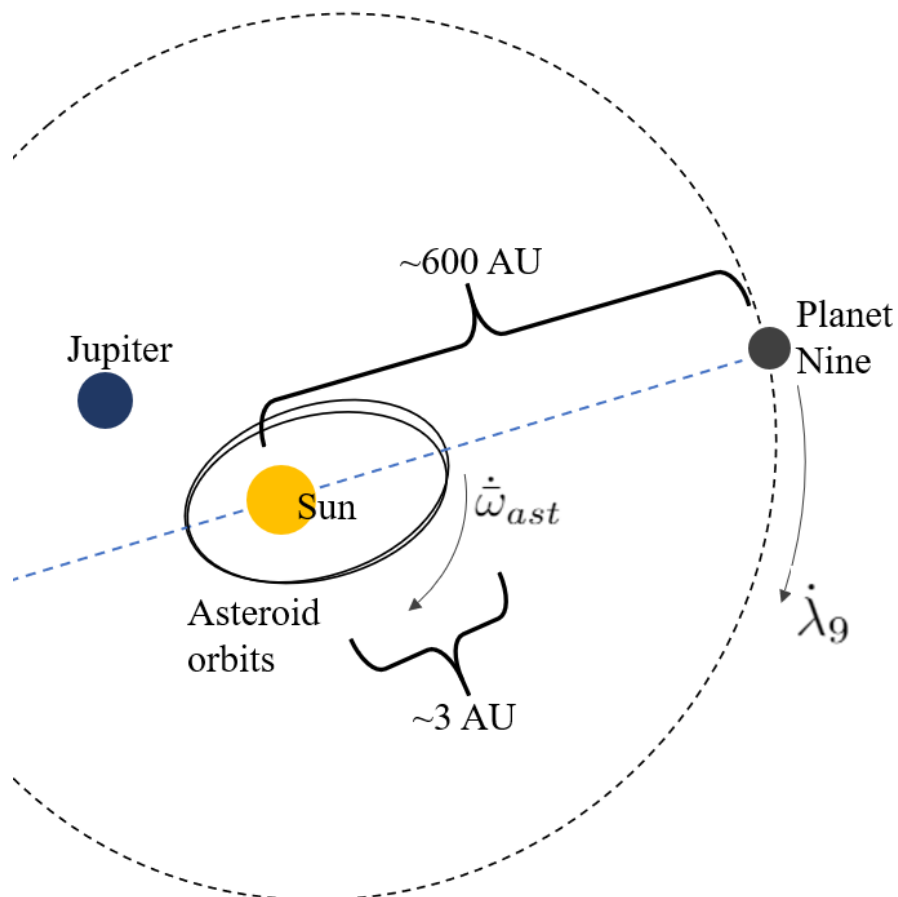


Figure 1.1: A sketch on the geometry of the investigated system, where the angle $\bar{\omega}_{ast} - \lambda_9$ is librating around a fixed value due to the asteroid being captured into orbital resonance.

1.4 Orbital Resonance

The mechanism upon which this project is based is orbital resonance. This resonance is a phenomenon between the orbits of certain bodies in a many-body system possible to occur when two frequencies of the system are close. In the case of our

project, they are the apsidal precession of an asteroid and the orbital frequency of Planet Nine.

We consider a Sun-planet-asteroid model. In this case, the perturbation by the planet causes the apsidal precession in the asteroid. With each conjunction of the asteroid and planet, they exert a gravitational force on each other and the less massive asteroid is perturbed from its previous orbit. At any moment, the orbit of the asteroid is described by its osculating elements and these elements are a function of time. For example, the perturbations cause the longitude of perihelion ($\bar{\omega}$) to change. The rate of change can be described by a precession frequency ($\dot{\bar{\omega}}$). This rate is usually much smaller than that of orbital mean motion and is thus called "secular". Analytically, it can be expressed as

$$\dot{\bar{\omega}} \propto C + K \cdot \cos(\bar{\omega} - \bar{\omega}') \quad (1.3)$$

where C, K are constants, dependent on the masses and orbital elements of the involved objects, and $\bar{\omega}'$ is the longitude of perihelion for the perturbing planet Murray and Dermott (1999).

At this point, it is necessary to introduce another variable of the orbit. An object in orbit has an angular position measured from the reference direction. This is called the mean longitude λ and is the sum of the mean anomaly and the longitude of perihelion. The velocity by which λ changes, $\dot{\lambda}$, is then the average angular velocity of the planet in its orbit. If the precession of an asteroid (1.3) is close to the mean motion ($\dot{\lambda}_{res}$) of another body, i.e

$$\dot{\bar{\omega}} \approx \dot{\lambda}_{res}, \quad (1.4)$$

it can enter orbital resonance. The object with mean motion $\dot{\lambda}_{res}$ in resonance with the asteroid can be the perturbing planet, as denoted by a ' as in equation (1.3), or an additional planet in the system. For such systems locked into orbital resonance, the perihelion of the asteroid is locked to the position of the object in resonance, and the critical angle $\bar{\omega} - \lambda_{res}$ will librate around a fixed value Yokoyama et al. (2008).

A previously studied mechanic of this kind is the evection resonance. In this canonical evection resonance the asteroid or other small body is driven into precession by the same object that it enters resonance with, meaning that the parameters denoted by a ' in equation 1.3 are for the same object as $\dot{\lambda}_{res}$ in equation (1.4). However, the perturber must be very massive to drive the precession fast enough to match the mean motion $\dot{\lambda}_{res}$. For instance, the Sun acted as both the perturber causing the precession of a satellite around Jupiter and the object with an orbital period in resonance with the precession of the satellite. For this case, the critical angle $\bar{\omega} - \lambda_{\odot}$ may librate around 0° or 180° and the satellite's eccentricity is forced to oscillate Yokoyama et al. (2008). We remember, as stated before, that the

precession and resonance are not necessarily due to the perturbation of the same object. In another system similar to the one just mentioned above, the satellite's precession was mainly driven by the oblateness of Jupiter whilst still in resonance with the Sun Frouard et al. (2010).

The system of our paper has a geometry, as seen in figure 1.1, that is different from both of these. Our system contains four objects: the Sun, Jupiter, an asteroid and Planet Nine. In actuality, there is a large number of asteroids but these affect each other only a negligible amount. As such, we can view the system as many single-asteroid systems. The orbit of the asteroid secularly perturbed by Jupiter has a precession frequency $\dot{\bar{\omega}}_{ast}$ close to the mean motion $\dot{\lambda}_9$ of Planet Nine, so the asteroid may enter orbital resonance with it. The angle $\bar{\omega}_{ast} - \lambda_9$ may then librate around fixed values, and the perihelion will be locked to the position of Planet Nine. For ease of reference for our specific system of orbital resonance, where Jupiter determines the apsidal precession of the asteroid while the resonance is directly related to Planet Nine, we will call it **P9AJER** (Planet Nine-Asteroid-Jupiter Evection Resonance) for the remainder of the project.

In the following pages of this project, we will first investigate the apsidal precessions of asteroids in the Main Belt. With their motions known, we will introduce a Planet Nine to our simulations in the parameter space where resonance may occur. Lastly is a discussion concerning the applicability and future studies of our investigated mechanism.

Chapter 2

The Main Asteroid Belt with Jupiter as Perturber

In order to investigate the conditions for our resonance, the precession rates of the asteroids must be known. An analysis on the precessions of simulated asteroids was thus made in the semi-major axis range of 2.5 - 3.5 AU. From this initial analysis, a smaller range of semi-major axis for the asteroids will be chosen for the simulations including a ninth planet.

Jupiter was assumed to exert the greatest effect on the precession of the asteroids. As such, our system contains asteroids in orbit around the Sun along with only the perturbing body of Jupiter. Omitting the other planets of the Solar System drastically reduces the number of bodies, and subsequently the number of computations, in the simulation. This also removes a large number of possible mean motion resonances with the rocky planets and the only resonances that could occur were with Jupiter.

The simulation software used was the *Mercury* program, a fortran N -body integration package Chambers (1999). *Mercury* differentiates between "big" and "small" bodies. Big bodies interact and affect all other bodies in the system, while small bodies interact only with big bodies and not between themselves. For this simulation, all asteroids were set as massless small bodies.

2.1 Numerical simulations

To determine the precession rates of asteroids perturbed by Jupiter, we performed an N -body integration using the *Mercury* software. We adopted the current orbit of Jupiter in the simulation. 1000 massless asteroids were given evenly distributed semi-major axes in a range from 2.5 to 3.5 AU. Their eccentricities and inclinations were randomly generated, with the eccentricities within $(0, 0.01)$. Inclinations were

distributed between 0° and 1° with respect to the jovian orbital plane. While all of the Main Asteroid belt is not this flat, many asteroids lie in this range.

All other angular orbital elements were randomly set as any value in their full range. This system of Sun, Jupiter and 1000 asteroids is integrated for 2×10^6 years. From the integration data, the orbital elements for each body evolving over time were extracted in order to be analysed.

2.2 Data Analysis & Plotting

From the orbital elements for each asteroid, the precession period was found via a Fast Fourier Transform (FFT). The FFT was carried out on a two-component time series using the terms $e \cos \bar{\omega}$ and $e \sin \bar{\omega}$ as input, where e and $\bar{\omega}$ are the eccentricity and longitude of perihelion respectively for each asteroid. The sine- and cosine-expressions of the longitude of perihelion allowed the transform to find the rotational frequency of the angle. As the asteroid eccentricity varies in correlation with the longitude of perihelion, it was included in the terms in order to gain stronger results Murray and Dermott (1999).

The result of the FFT analysis of an example asteroid is shown in figure 2.1. There we observe the strength's sensitive dependence on the corresponding period. In this case there is a strong peak at 15000 yr, the period at which the the longitude of perihelion precesses. This peak frequency is then picked out for all asteroids. As the asteroids were distributed evenly over a span of semi-major axis, the precession period of each asteroid corresponds to the precession period of an object at that semi-major axis. With both the data for the semi-major axis and the period of precession given by the FFT, we can plot the relation between them, as is shown in figure 2.2. An explanation for the behaviour of the plot follows in the next section.

Another integration simulating asteroids on orbits with larger semi-major axes for the asteroids was performed. For this investigation, the axes ranged from 3.0 to 3.8 AU. As in the analysis of the asteroids with smaller semi-major axis, the periods of precession were coupled to the semi-axes of the asteroids. These results are shown in the appendix in figure A.1.

2.3 Interpretation

As seen in figure 2.2, the period of precession decreased from over 25000yr to less than a few 1000yr with an increasing semi-major axis as the asteroids approach Jupiter and the perturbing force grows. The decrease in period continued to a semi-major axis of approximately 3.3 AU, where the 2:1 mean-motion resonance

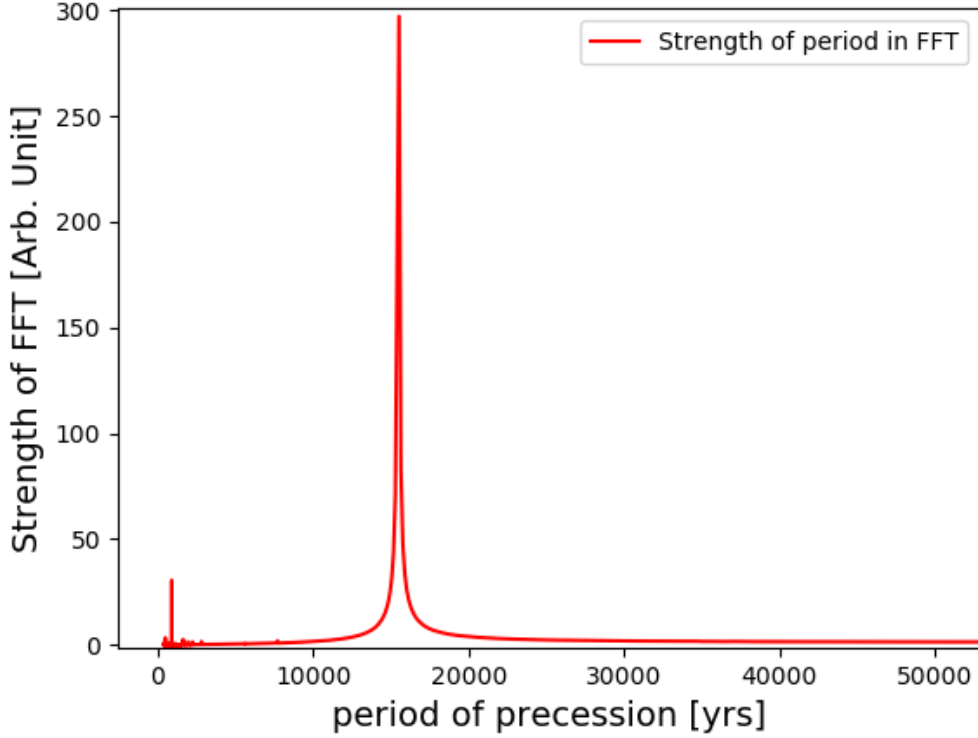


Figure 2.1: The strength of the FFT carried out on the varying longitude of perihelion along with the eccentricity of the orbit.

with Jupiter occurs Gallardo (2006). At this 2:1 resonance, the orbits of the asteroids were highly disturbed by the resonant interactions and this explains the chaotic behaviour of the asteroid precession periods there.

For the investigation of our resonances, we need to find a semi-major axis largely free from mean-motion resonances in figure 2.2. Beyond 3.3 AU, as seen in figure A.1 in the appendix, the precession periods behaved more unstable due to the large number of mean-motion resonances with Jupiter present Gallardo (2006). As such a smaller semi-major axis than 3.3 AU is needed for the further investigation.

Our resonance relies on the agreement between the asteroid's precession period P_{ast} and the orbital period of Planet Nine T_9 . Thus the latter, apparently dependent on its semi-major axis a_9 , would also affect our choice of the semi-major axis of the asteroid a_{ast} . Capture into orbital resonance in our investigated system may occur only when the asteroid's velocity of longitude of perihelion $\dot{\omega}_{ast}$ is close to the mean motion $\dot{\lambda}_9$ of Planet Nine. This means that any Planet Nine added to

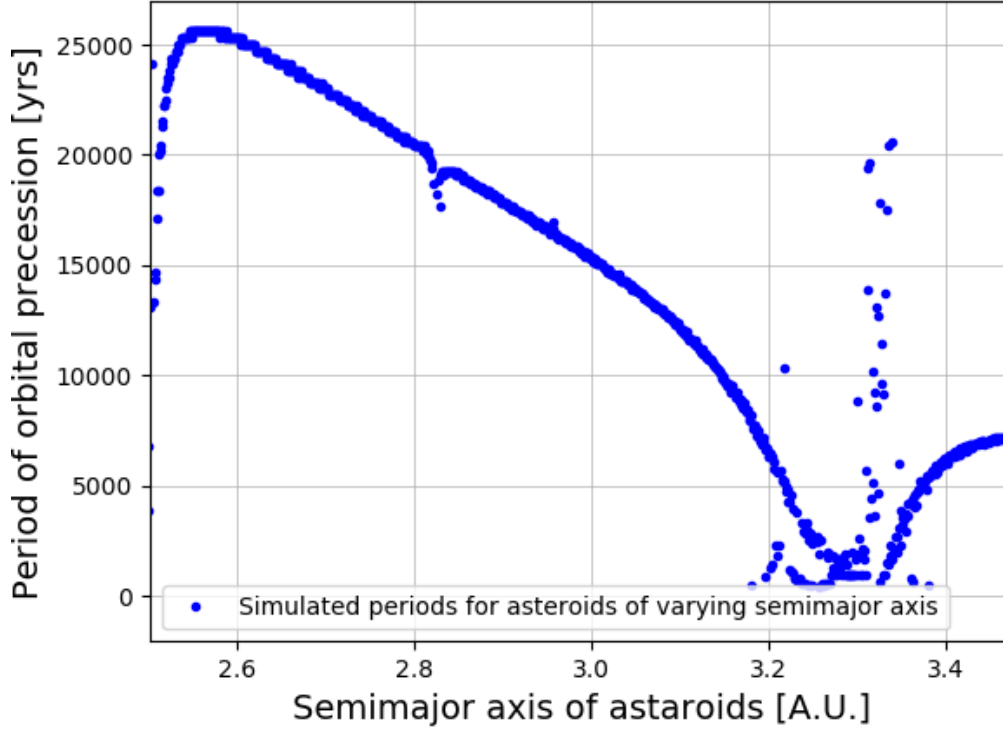


Figure 2.2: The period of precession for asteroids in the span 2.5-3.5 AU. The asteroids are massless bodies orbiting the sun in a system perturbed only by Jupiter.

the simulated system must have a semi-major axis giving it a period close to the precession period. The correlation between the semi-major axis a_9 and the period T_9 is, according to Keplers third law:

$$\frac{a_9^3}{T_9^2} = \frac{a_9^3}{P_{ast}^2} = G \frac{M_\odot + m_9}{4\pi^2} \approx G \frac{M_\odot}{4\pi^2}, \quad (2.1)$$

where P_{ast} is the asteroid's apsidal precession period. The above approximation holds only when the mass of Planet Nine (m_9) is negligible in comparison to the mass of the Sun (M_\odot). From equation (2.1) it is seen that a shorter precession period corresponds to a smaller semi-major axis of Planet Nine than that for a larger period. With increased distance between the interacting objects, the strength and subsequent probability of capture into orbital resonance would decrease Yokoyama et al. (2008).

With respect to the above points, we chose a semi-major axis of 3.0 AU for the asteroids, free from strong mean-motion resonances with Jupiter. For this distance,

the precession period is determined from the correlation in figure 2.2 as ~ 15300 yrs. Under the requirement that the period of Planet Nine is approximately equal to the precession period, equation (2.1) yielded a semi-major axis of Planet Nine of ~ 600 AU, which is consistent with the estimated value Batygin et al. (2019).

Chapter 3

Planet Nine Simulations

With the behaviour of the asteroids known, a Ninth Planet was added to the list of "big" bodies alongside Jupiter. The new orbital system was then analyzed in search of our Planet Nine-Jupiter-Asteroid Evection Resonance (**PP9AJER**). See figure 1.1 for an illustration of the system.

3.1 Parameters of Planet Nine

As discussed in Section 2, the apsidal precession period of the asteroids are dependent on their semi-major axis. For asteroids of a certain semi-major axis, they can enter **PP9AJER** if the orbital period of the planet is very close to the precession period. For this to occur, we can use equation (2.1) to find a suitable semi-major axis for Planet Nine. However, in the Newtonian equation of motion the mass of Planet Nine has to be known first. Earlier studies of Planet Nine have suggested a mass between five and ten Earth masses Batygin et al. (2019).

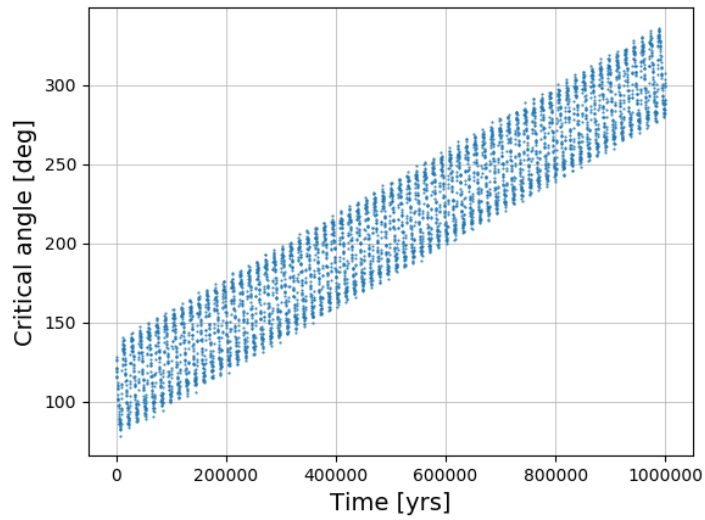
As a larger mass exerts a larger gravitational effect, a mass of Planet Nine larger than that estimated by other studies yields a stronger probability of **PP9AJER** occurring. In the initial *Mercury* simulation carried out with Planet Nine, the planet was given a larger mass of 1000 Earth masses ($1000m_{\oplus}$). Such a massive planet is implausible as it would probably already be detected. If simulations with the increased mass can result in resonance, the mass could be decreased and approach the more reasonable values.

With the mass of Planet Nine set to $1000m_{\oplus}$, the semi-major axis could be determined via equation (2.1). Even in the case of this mass, the effect of the mass of Planet Nine on the calculation of its semi-major axis is negligible. The resulting value is 629.9 AU. Other studies have concluded that a possible Planet Nine would have a semi-major axis in the range of 400 - 800 AU Batygin et al. (2019), so our semi-major axis is consistent with the estimate.

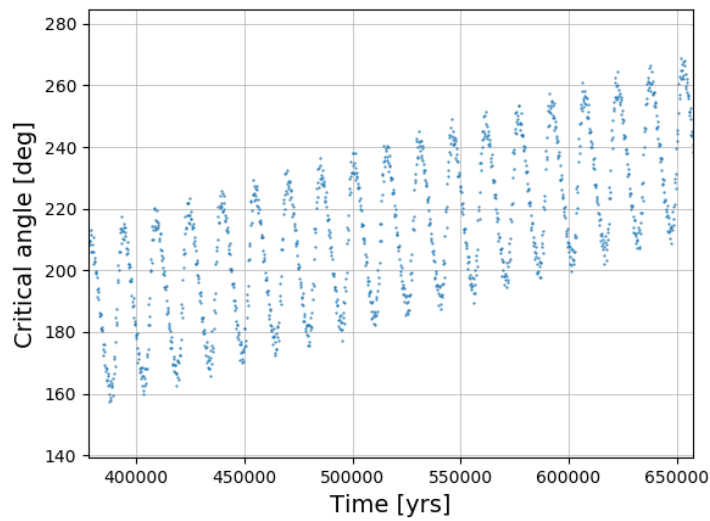
Besides the semi-major axis and mass of Planet Nine, other parameters had to be set before the simulations could be carried out. We have set the inclination of Planet Nine to be zero. The implemented inclination does not agree with other studies that indicate values between $15 - 25^\circ$, but by reducing the problem to a coplanar one any complexities involving the z -direction are eliminated. The value for the input eccentricity of 0.2 better agrees with the current hypothesis of Planet Nine. As all input parameters for Planet Nine were determined, the simulation of the system including the additional planet could begin.

3.2 Simulations over one million years

With the parameters for Planet Nine set, integrations were carried out over a period of one million (10^6) years. Over this timespan, the orbits of 100 asteroids were then analyzed in search for **P9AJER**. The asteroids were evenly placed in the range 2.990-3.004 AU, with initial eccentricity set to 0.1 and inclination below 1° . An example output is shown in figures 3.1a and 3.1b, for the asteroid with precession period closest to the orbital period of Planet Nine.



(a) Time evolution of the critical angle, the angle between the mean longitude of Planet Nine and the longitude of perihelion of an asteroid. This asteroid has an initial semi-major axis of 2.997 and eccentricity of 0.1. Planet Nine is at a semi-major axis of 619.900 AU.



(b) A zoomed-in view of (a). The oscillations have a period of approximately 15 000-16 000 years.

Figure 3.1: Time evolution of the critical angle for the asteroid in the 1 Myr simulation with a precession period closest to the orbital period of Planet Nine.

In figure 3.1a, the critical angle is seen to traverse the full range of 0° - 360° . It also oscillates with a period much smaller than the full integration timespan of 10^6 years. The oscillations, seen more clearly in figure 3.1b, seem to have a period matching the precession period of the asteroid. By comparison with the expression of equation (1.3), the oscillations are explained as caused by the perturbations by Jupiter. In the equation the period depends on the period of $\bar{\omega} - \bar{\omega}'$. As the longitude of perihelion for Jupiter varies much more slowly than that of the asteroids, the oscillations have the same period as the asteroids. A short code script identified asteroids with a critical angle that did not pass the full 360° during a set timespan. We then visually checked the time evolution of the critical angle for these asteroids, that have a precession period closest to Planet Nine's orbital period. None of the asteroids' critical angles are librating.

3.3 Simulations over twenty million years

One possibility for the non-detection of **P9AJER** is that the timescale of the simulation was too short. To investigate whether a longer integration time could yield a positive result, the simulation of the same system was extended to 20 million years. The same analysis as for the shorter simulation was performed. An example is presented in figure 3.2 for the same asteroid as in figure 3.1, for which the precession period is closest to the orbital period of Planet Nine among all our asteroids. Similar to the shorter integration, the critical angle passed over the full 360° without any indication of libration around any fixed value and thus no capture into orbital resonance was observed.

In the canonical evection resonance when near or in resonance, the evolution of the eccentricity is strongly coupled to the evolution of the critical angle Yokoyama et al. (2008). As a result, the two parameters evolve on similar timescales. In order to investigate the possibility of **P9AJER**, the eccentricity of the asteroids was also plotted against the simulation runtime in search of an evolutionary trend on the same timescale as that of $\dot{\bar{\omega}}_{ast} - \dot{\lambda}_9$. As example is presented in figure 3.3, which only shows oscillations on a short timescale. No indication of the asteroid being momentarily captured into orbital resonance was thus found through the investigation of the asteroid's eccentricity.

3.4 Resonance strength

In the system simulated above, for timespans of both one and twenty million years, no libration in the critical angle for **P9AJER** is observed. Whether or not capture into resonance occurred is dependent on the resonance strength/width. In order to

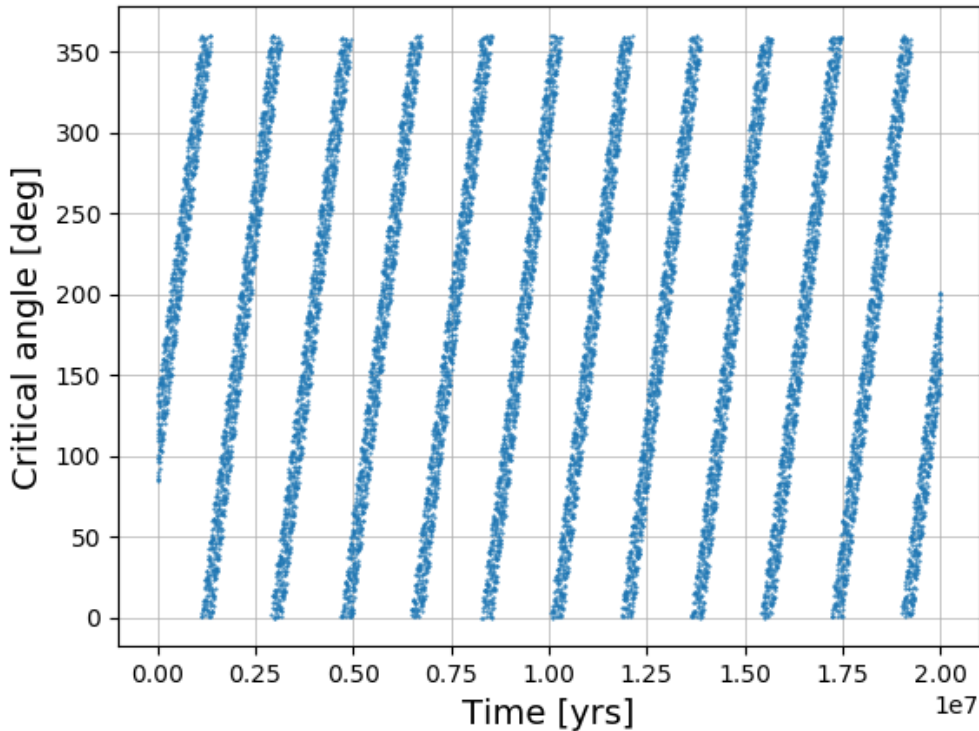


Figure 3.2: Time evolution of the critical angle for the asteroid in the 20 Myr simulation with a precession period closest to the orbital period of Planet Nine.

change the parameters of the system so that resonance has a higher probability to occur, the correlation between the resonance strength and Planet Nine parameters needed to be known.

A paper by Yokoyama et al. (2008) studied the canonical evection resonance. Unlike the system in this project, their paper studied one where the perturbed body is a satellite of Jupiter. Their perturbing body was the Sun, which has a perturbing mass larger than that of Planet Nine, as used in the simulations in Sections 3.2 and 3.3 by several orders of magnitude. Yokoyama et al. showed the strength S of the orbital resonance, where we have modified the expression to suit our project, to be

$$S \propto \frac{m_9 a^2}{a_9^3} e^2 \cos(2\bar{\omega}_{ast} - 2\lambda_9), \quad (3.1)$$

where the subscript 9 denotes the parameters of Planet Nine for the system of this project and a, e are the semi-major axes and eccentricities for the asteroid respectively. As seen from the equation, the ratio of the two semi-major axes

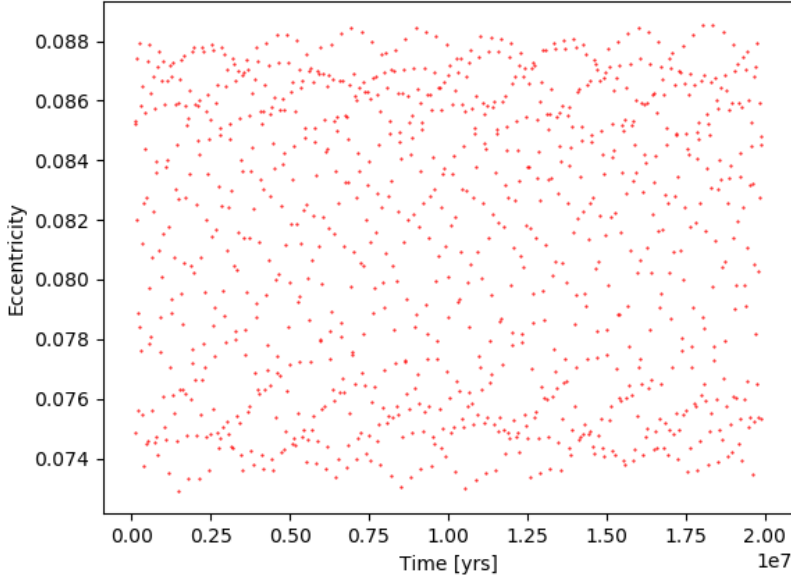


Figure 3.3: Time evolution for the eccentricity of the same asteroid as in figure 3.2 from the 20 Myr simulation.

affects the strength of the resonance. In comparison with the paper by Yokoyama et al., where the Sun was seen as the perturbing body with a semi-major axis of only a few AU, the used semi-major axis of Planet Nine fulfilling the resonance condition was hundreds of times greater.

We now do a back-of-the-envelope calculation to compare the resonance strength of our project with that in Yokoyama et al.’s paper. The strength ratio is, for the above adopted parameters of Planet Nine, approximately

$$\frac{S_{P9}}{S_{Yokoyama}} \sim \frac{\frac{m_9 a^2}{a_9^3}}{\frac{M_{\odot} a'^2}{a_{\odot}^3}} \approx 4 \cdot 10^{-7}. \quad (3.2)$$

In the equation above, a and a' respectively are the semi-major axes of the asteroid and that of the satellite around Jupiter, the different perturbed bodies our and their work. As seen, the strength of the resonance with Planet Nine is orders of magnitude weaker than that in the paper by Yokoyama. So it is likely that the non-detection of **P9AJER** in the simulations carried out so far stems from the fact that **P9AJER** is too weak for those parameter choices. In order to produce an observable capture into resonance the parameters of the system needed to be changed in favour of stronger interaction.

3.5 Migrating Planet Nine

One method to increase the probability of capture is to let Planet Nine migrate over a region of semi-major axis. When migrating, the orbital period of the planet changes. As such, the resonance period will sweep over a range of semi-major axes for the asteroids. One study showed that probability of capture depends on the rate of migration. A slower migration yields a higher capture probability compared to a faster migration Xu and Fabrycky (2019).

We choose Planet Nine as the body to migrate in our simulations. Migration of the asteroids or Jupiter would also increase the chance of resonance capture, but in that case the apsidal precession period would be changed in a way not easily determined. For a migrating Planet Nine, the corresponding orbital period is easily calculated with equation (2.1). Planet migration is a phenomena with evidence in other studies. Simulations with Planet Nine in a gas disk have shown the planet might migrate inwards Bromley and Kenyon (2016). Another study also shows that a high-eccentricity Planet Nine can decrease in semi-major axis due to interaction with planetesimals far beyond Neptune Eriksson et al. (2018). In both studies, if the disk is long-lived, the migration has a timescale of ~ 100 Myr - 1 Gyr Bromley and Kenyon (2016).

The direction of the migration may affect the probability of capture into orbital resonance. In principle, capture into resonance should only be possible for one direction of migration, depending on the phase-space structure of the resonance Xu and Fabrycky (2019). In our case, however, we do not know the direction that should allow for capture. As such, we decide to migrate Planet Nine in both directions, but present in detail only the instances of **P9AJER** from the inward migration. The implementation of the migration, as well as our other parameter changes, are detailed below.

3.5.1 Solar-massed Planet Nine simulations

To make Planet Nine migrate, we use a version of *Mercury* modified by Joseph Hahn Hahn and Malhotra (2005). The change of a_9 roughly follows

$$a_9 = a_0 - \alpha \cdot e^{-(t/\tau)}. \quad (3.3)$$

Here a_0 is the initial semi-major axis of Planet Nine, and the semi-major axis a_9 at any time exponentially changes with α . τ and t are the timespan of the migration and the simulation time respectively. From Section 3.4, it is apparent that the strength of the resonance was too weak to allow for capture into orbital resonance. Hence, along with migrating Planet Nine, the mass of Planet Nine was also increased to a solar-mass in order to improve the chance of capture into resonance. The change of Planet Nine's mass causes a non negligible change in

semi-major axis of Planet Nine in accordance with (2.1), where the resulting distance is ~ 777.2 AU. We decreased the number of asteroids in the simulation to 20 to save CPU-time for this integration.

Over the timescale of 50 Myr, Planet Nine decreased in semi-major axis by 20 AU. Similar to before, we plot the time evolution of the critical angle for an example asteroid in figure 3.4. The critical angle for the asteroid and Planet Nine does not span the full 360° , but librates around $\sim 90^\circ$ and $\sim 270^\circ$. Interestingly, the critical angle for this asteroid transitions between librating around 90° and 270° . This behaviour of the critical angle indicates capture into **P9AJER** meaning that for these parameters of Planet Nine, it would be possible to detect it from the dynamics of asteroids.

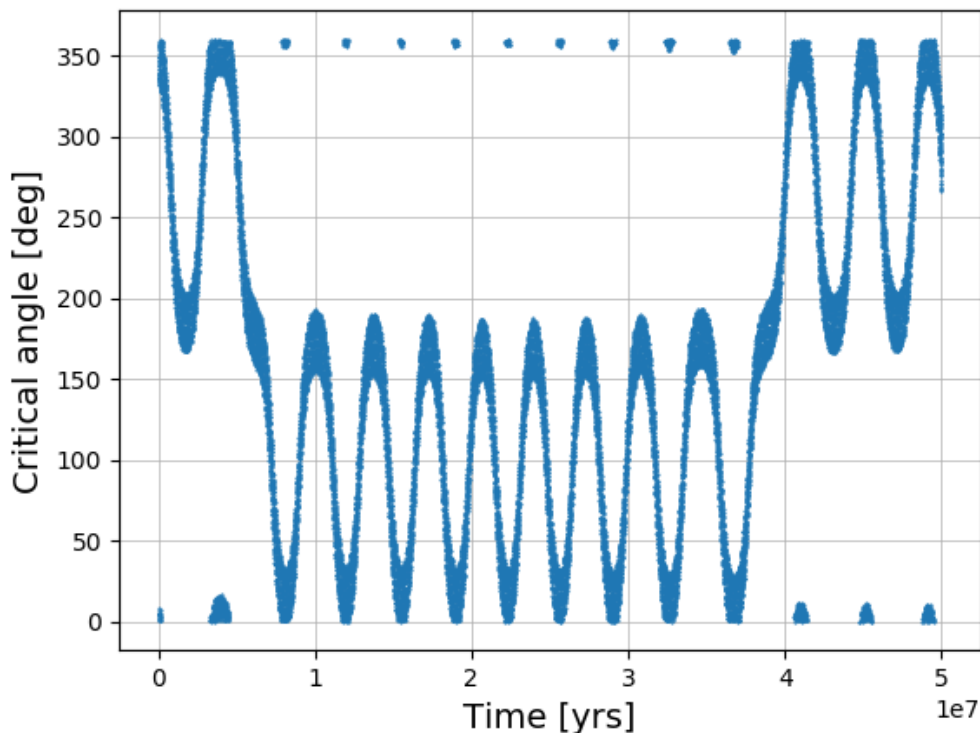


Figure 3.4: Time evolution of the critical angle of an asteroid in **P9AJER** with a solar-mass Planet Nine as the planet migrates inwards.

From the observed instance of libration in figure 3.4, a phase-space diagram can be constructed. In practice, we plot the variables $(e - 0.05) \cos(\bar{\omega}_{ast} - \lambda_9)$ against $(e - 0.05) \sin(\bar{\omega}_{ast} - \lambda_9)$ of the asteroid in figure 3.4. The colour of a data points corresponds to the time in the simulation and the evolution over time can

thus be seen. In order to better show the resonance structure the eccentricity was offset by 0.05.

Figure 3.5 shows the critical angle of the orbital resonance to librate around $\cos(\bar{\omega}_{ast} - \lambda_9) = 0$ and $\sin(\bar{\omega}_{ast} - \lambda_9) = \pm 1$, which corresponds to $\bar{\omega}_{ast} - \lambda_9 = 90^\circ, 270^\circ$. The time evolution of the critical angle shows the asteroid to have transitioned between these two resonance angles. Inclusion of the asteroid’s eccentricity shows that, as previously mentioned, its behaviour is coupled to that of the longitude of perihelion. Along with the data from the libration case of figure 3.4, we also plotted data for a non-resonance asteroid, as shown in red \times :s. For this, the critical angle shows circulation over the full 360° .

Yokoyama et al. derived the phase-space structure of the canonical evection resonance and found libration not around our resonant angles, but around 0° and 180° Yokoyama et al. (2008). This is unsurprising and can be explained by the difference in the structure of resonance for our work and that by Yokoyama et al.

In the canonical evection resonance, the resonance system contains a planet with associated satellite and the Sun. For this case, the Sun is both what drives the satellite’s apsidal precession and is the body with the mean longitude λ in resonance with the precession. However, in **P9AJER**, Jupiter drives the precession of the asteroid while the λ of Planet Nine is involved in the resonance. We note that in a situation close to the canonical evection resonance, where the oblateness of the planet is taken into consideration, it may dominate the satellite’s precession. As a result, the libration centres can be the same as for **P9AJER** Frouard et al. (2010).

Including the case of libration in figure 3.4, out of the 20 simulated asteroids, four cases of libration were observed in the simulation. They all had semi-major axes within $[2.99547, 2.99863]$ AU, and librated around either 90° or 270° . Interestingly, all of the asteroids exhibit libration from the very start of the simulation. Thus we do not know if they are captured into resonance, in which case the critical angle should first circulate then librate.

It is also possible for a planet to increase in semi-major axis. By exchanging angular momentum with a planetesimal disk, Neptune is believed to have migrated outwards and increased its semi-major axis by at least ~ 5 AU Hahn and Malhotra (2005). Another simulation was then performed where we set Planet Nine to migrate outwards. Except for the direction of migration, all other parameters were the same as for the inward migration. According to the previous mentioned study, capture into resonance should only be possible for one direction of migration Xu and Fabrycky (2019). No libration behaviour should then be observed for outward migration. But as seen in figure A.2 in the appendix, libration does occur in our simulation for outwards migration. The details of why this occurs, contrary to what we expect, are discussed in chapter 4.

3.5.2 Simulations with one tenth solar-mass

Given that **P9AJER** is observed in our simulations for a Planet Nine of a solar mass, we now proceed to explore a relatively more plausible mass for the planet: one tenth of a solar mass. The new semi-major axis, for which the planet has a period close to the asteroids' precession period at 3 AU, was calculated with equation (2.1). All other parameters of the system were kept as in the previous simulations.

We performed two separate simulations: one for each direction of migration. In the case of outward migration of Planet Nine, we observe a librating behaviour as seen in figure 3.6a. The critical angle initially librates around $\sim 80^\circ$. However, over the course of the simulation, the libration shifts to be centered around $\sim 90^\circ$ which is more consistent with the libration angles of the solar-mass simulations. Apart from the asteroid in figure 3.6a, one more asteroid displays libration. It too shows the same shift of the libration angle. Both asteroids are initially trapped in **P9AJER** and do not transition from circulation to libration.

Despite observing **P9AJER** in the case of outward migration, there is no libration for asteroids with a Planet Nine of one tenth solar mass that migrates inward. Figure 3.6b shows the time evolution of the critical angle for an asteroid in the simulation. Due to the migration and subsequent changing of Planet Nine's orbital period, it is at one point equal to the asteroid's apsidal precession period. This occurred $\sim 20\text{Myr}$ into the simulation, and despite capture into **P9AJER** being most probable at this point no asteroid out of the 20 simulated was captured.

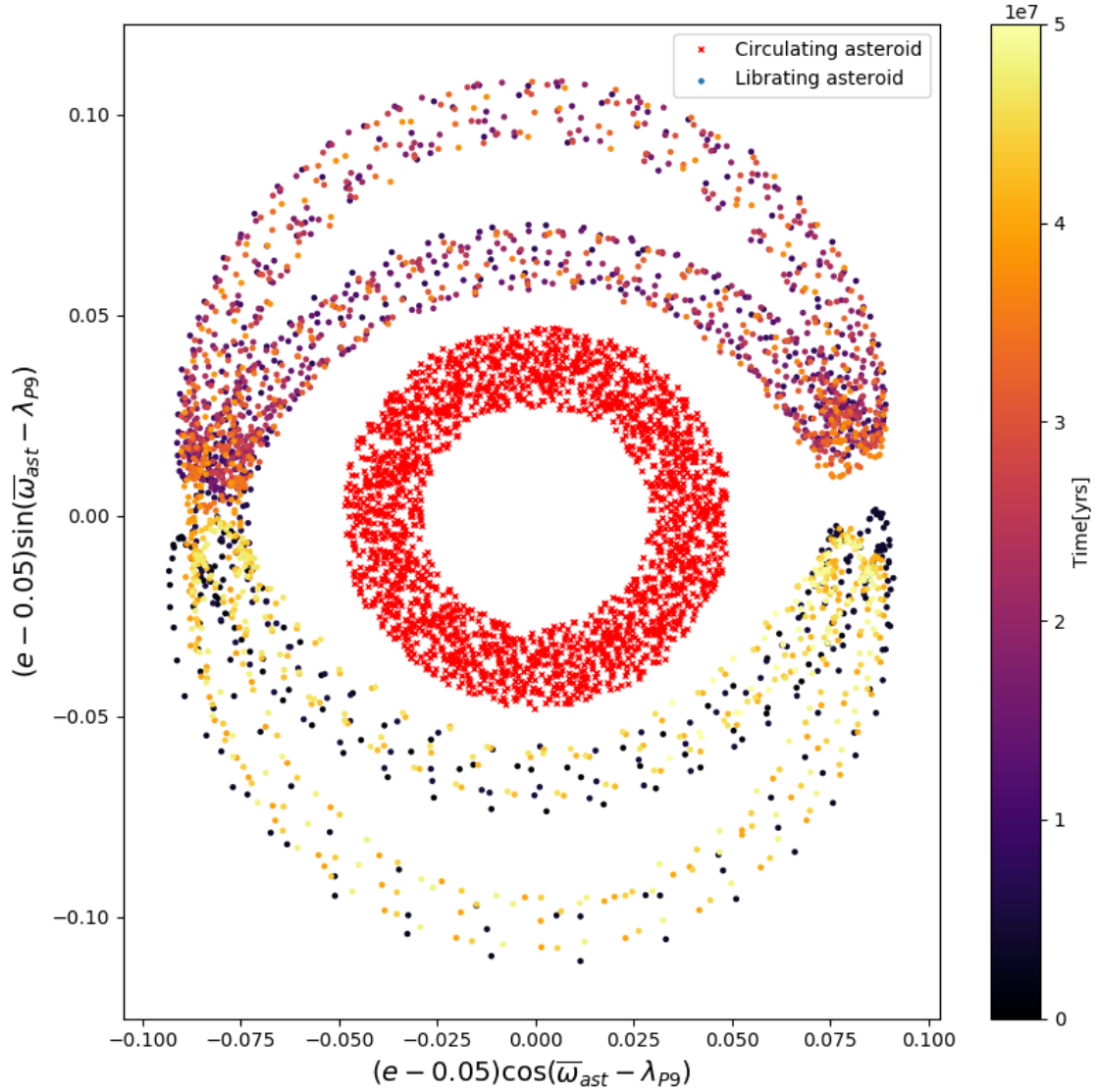
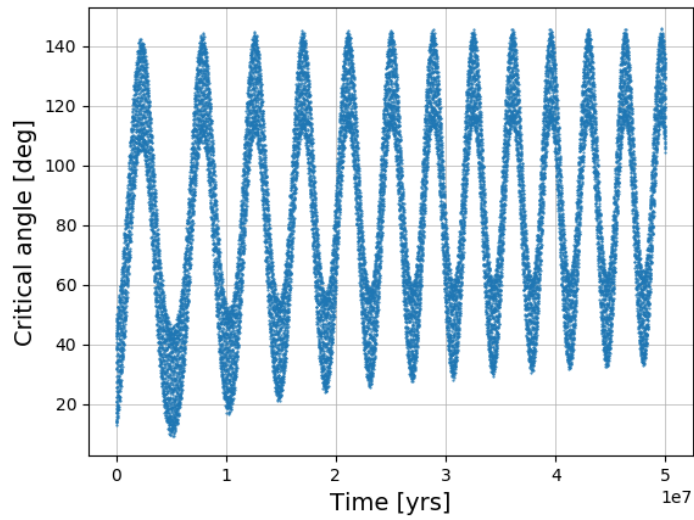
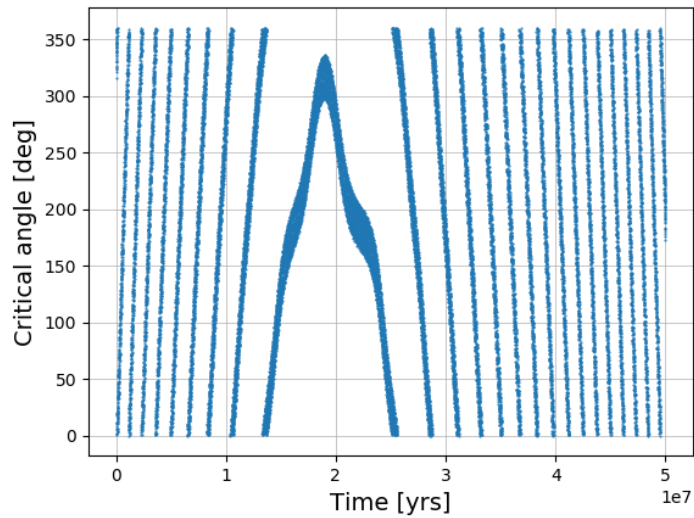


Figure 3.5: Phase-space diagram of the critical angle and eccentricity for two asteroids, one in **P9AJER** (coloured circles) and one in circulation (red crosses). The data for the librating asteroid is from the same asteroid as in figure 3.4, and for this case the colour gradient of the data points correspond to the integration time of the specific values.



(a) Time evolution of the critical angle in a system where Planet Nine migrates outwards. The data is for an asteroid with a semi-major axis initially at 3.0076 AU in **P9AJER**.



(b) Time evolution of the critical angle in a system where Planet Nine migrates inwards. At approximately 20 Myrs, the period of Planet Nine and the apsidal precession of the asteroid are equal, but no capture into **P9AJER** is observed.

Figure 3.6: Time evolutions of the critical angles for the asteroids in a system containing a migrating Planet Nine, with one tenth of a solar mass, simulated for 50Myr.

Chapter 4

Discussion & Conclusion

In this project, we have attempted to find out whether a Planet Nine could capture Main Belt asteroids into a specific type of orbital resonance, which we refer to as **P9AJER** (Planet Nine-Asteroid-Jupiter Evection Resonance), by simulating the system in the N -body simulator *Mercury*. In this resonance the apsidal precession of an asteroid, driven by Jupiter, is close to the orbital period of Planet Nine. However, the scope of such a question is too large to explore completely within the scope of his project. Here we will discuss the implications and limitations of this project and present our conclusion.

The greatest discrepancy between our adopted and the inferred value is the mass of Planet Nine. In order to produce orbital resonance, we have made it solar-mass or a tenth of a solar mass. Given that the estimate is up to ten Earth-masses Batygin et al. (2019), we increased the mass approximately by a factor of 3×10^4 . A planet of solar-mass would, naturally, begin fusion and be our closest and brightest star. Its effect on other objects of the Solar System, such as distant Kuiper Belt objects, would also be much stronger than for the observed asteroids we studied. So for future investigation to be more realistic, it is a must to consider a sub-stellar mass for Planet Nine. Though we, in our limited parameter space, detect no resonance for such masses (we tested only one such scenario, 1000 Earth masses), other combinations of Planet Nine's a, e, i could increase the chance of resonance capture. Furthermore, our study also assumed the asteroids of the Main Asteroid Belt to have nearly circular orbits with low inclinations. In actuality, the asteroids of the Main Belt are highly excited, with eccentricities over 0.2 and inclinations up to tens of degrees Murray and Dermott (1999). As the strength S of resonance depends on the eccentricity e_{ast} as $S \propto e_{ast}^2$ Yokoyama et al. (2008) and we implemented an eccentricity up to 0.1, the strength of resonance could increase by a factor of 4. N.B.: In short, the parameters we have used are limited and actually implausible for the mass of Planet Nine. Future studies should explore wider ranges for the parameters where resonance may be observed.

While our mass values are clearly impractical, the adopted orbit for Planet Nine is more or less consistent with constraints from literature. In all simulations containing Planet Nine it was given an inclination and eccentricity of 0° and 0.2 respectively. While the eccentricity we adopted lies within the estimated range Batygin et al. (2019), the inclination is believed to be $\sim 15^\circ$ - 25° Batygin et al. (2019). Our choice of making the system coplanar was, by reducing the degree of freedom, to reduce the complexity of the problem. The semi-major axes used for the planet in the simulations all fall within the suggested value of 400-800 AU Batygin et al. (2019).

Another factor affecting the probability of capture in the case of the migrating Planet Nine is the rate of migration. We assume that, for a given set of parameters for Planet Nine, asteroids within a range Δa of semi-major axis may enter resonance with it. This Δa is apparently a function of Planet Nine's mass, where the more massive the planet the larger the Δa . As Planet Nine migrates, so does Δa , and the resonance sweeps through the asteroid belt at a rate of \dot{a}_{res} . If the migration of Planet Nine is slow enough that $\Delta a / \dot{a}_{res} > T_{lib}$, where T_{lib} is the libration period for the resonance, capture into resonance is highly likely. This means that while a smaller, more plausible, mass of Planet Nine results in a narrower Δa , making resonance less likely, a slower migration rate may counteract this and render libration possible.

According to analytical results, only one of two directions of migration should give rise to capture into resonance Xu and Fabrycky (2019). However, we observed libration in our simulations both for migrating Planet Nine in- and outwards. The reason for the unexpected resonances could be that the asteroid is not captured into resonance during the migration, but initial conditions are such that the asteroid is already in resonance at the beginning of the integration. This reasoning is supported by the fact that no instances were observed where an asteroid entered libration from circulation in the middle of the simulation. So in this sense, our migrating Planet Nine, designed to capture asteroids into resonance with a high likelihood, may be redundant and a stationary planet of solar mass may also trap asteroids easily. Neither for our simulations with Planet Nine having one tenth of a solar mass do we find a transition from circulating to librating.

If further studies take the above points into consideration, orbital resonance may be observed for numerical simulations with more probable parameters of Planet Nine. Such further studies could prove very useful in determining the position of the planet. Current studies constraining the parameters for Planet Nine have focused on the perturbation on the Kuiper Belt Objects (KBOs). However, only $\lesssim 2000$ are currently known Center, and out of those only about a dozen have wide enough orbits to be significantly perturbed by Planet Nine. Furthermore, the orbits of these objects are poorly known. In stark contrast to the

low number of such objects, millions of Main Belt Asteroids are numbered with orbits measured to a much higher accuracy. Apart from statistics, our method could produce information on Planet Nine not available via current studies. Most studies use secular perturbation from Planet Nine in order to constrain its orbit. Such a method, unlike ours, produces no information on the actual position of the planet. There have also been propositions of mean-motion resonances being used for constraining the orbit, but it was shown to be implausible to determine the position of the planet within the orbit Bailey et al. (2018). However, our method directly constrains the mean longitude of Planet Nine from the dynamics of the asteroids. Knowledge of Planet Nine’s position within the orbit could be used to inform the observational attempts to detect the planet.

In conclusion, we have found that asteroids within the Main Asteroid Belt, with an apsidal precession driven by Jupiter, can enter orbital resonance (**P9AJER**) with a Planet Nine positioned at a semi-major axis supported by the current hypothesis. The perihelion is then locked to the position of Planet Nine. For the resonances to occur, the planet needed to be of stellar mass. However, we only searched for **P9AJER** within a small range of (a, e, i) of Planet Nine, and combinations of these parameters untested by us may result in stronger resonance conditions. Thus, investigations in a larger parameter-space may find **P9AJER** possible for sub-stellar masses of Planet Nine. In order to more accurately constrain the parameters of Planet Nine for which it is possible, further studies are needed.

Acknowledgments

I want to express many thanks to my supervisor, Daohai Li, for all his insight, patience and advice. Others that have my utmost gratitude are several of my fellow bachelor students. Without their advice and support this work would be close to impossible.

Appendix A

Supplementary figures

For some of the performed simulations, the figures were not shown in the body of the thesis. These figures are supplementary to those in the thesis, and are as such presented in this appendix.

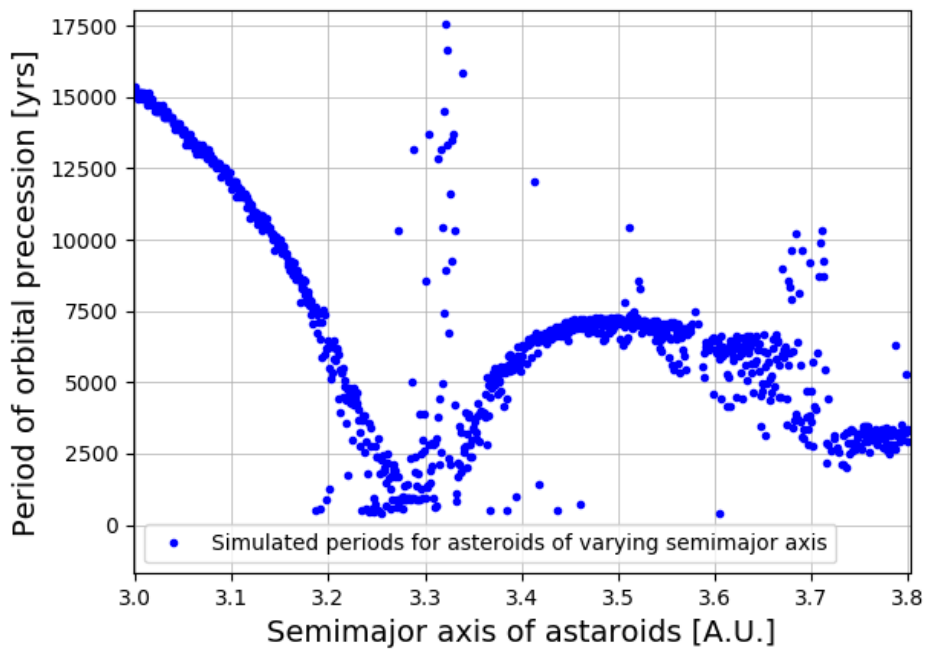


Figure A.1: Similarly to figure 2.2, the data points are precession periods for asteroids orbiting the sun perturbed by Jupiter, but the asteroids lie in the span 3.0-3.8 AU. For the outer asteroids, the orbits become highly unstable due to the proximity of Jupiter.

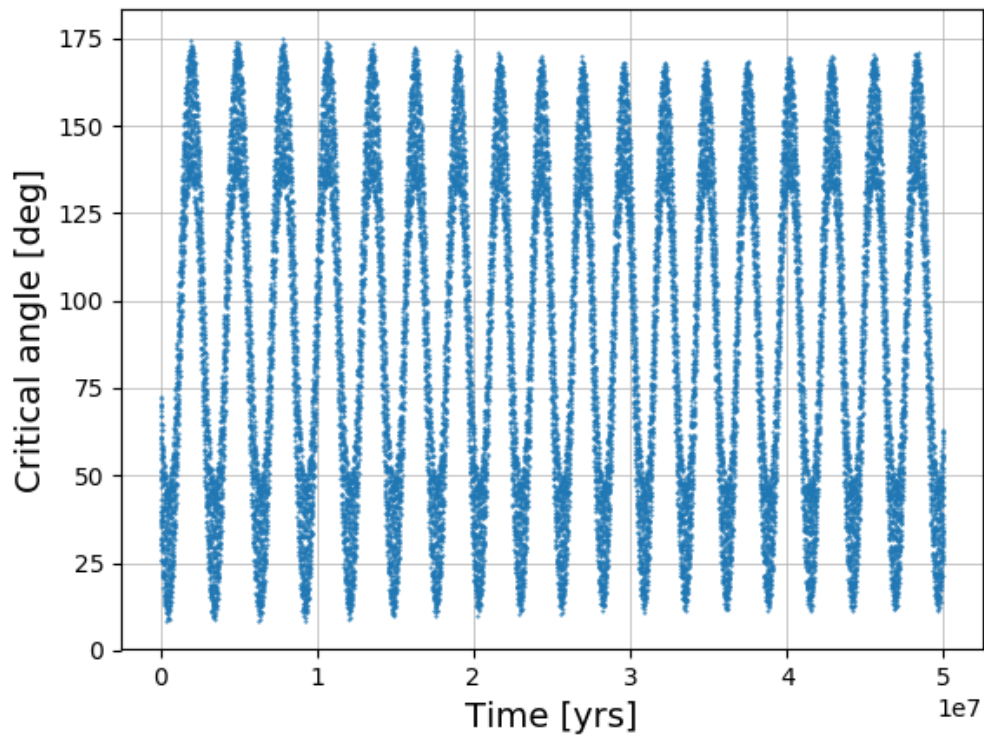


Figure A.2: Time evolution of the critical angle of an asteroid in the same system as 3.4, except Planet Nine migrates outwards. In this case, we observe the critical angle librating around $\sim 90^\circ$ and the asteroid is trapped into **P9AJER**.

Bibliography

- E. Bailey, M. Brown, and K. Batygin. Feasibility of a resonance-based planet nine search. *The Astronomical Journal*, 156(2):pp.6, 2018. doi: <https://doi.org/10.3847/1538-3881/aaccf4>.
- K. Batygin, F. Adams, M. Brown, and J. Becker. The planet nine hypothesis. *eprint arXiv*, page pp.92, 2019.
- B. C. Bromley and S. J. Kenyon. Making planet nine: A scattered giant in the outer solar system. *The Astrophysical Journal*, 826(1):pp.9, 2016. doi: https://ui.adsabs.harvard.edu/link_gateway/2016ApJ...826...64B/doi : 10.3847/0004 – 637X/826/1/64.
- T. I. A. U. M. P. Center. Data available from the minor planet center. URL <https://www.minorplanetcenter.net/data>.
- J. E. Chambers. A hybrid symplectic integrator that permits close encounters between massive bodies. *Monthly Notices of the Royal Astronomical Society*, 304: p.793–799, 1999.
- L. E. J. Eriksson, A. J. Mustill, and A. Johansen. Circularizing planet nine through dynamical friction with an extended, cold planetesimal belt. *Monthly Notices of the Royal Astronomical Society*, 475(4):p.4609–4616, 2018. doi: https://ui.adsabs.harvard.edu/link_gateway/2018MNRAS.475.4609E/doi : 10.1093/mnras/sty111.
- J. Frouard, M. Fouchard, and A. Viennem. About the dynamics of the evection resonance. *Astronomy Astrophysics*, 515:pp.11, 2010. doi: https://ui.adsabs.harvard.edu/link_gateway/2010AA...515A..54F/doi : 10.1051/0004 – 6361/200913048.
- T. Gallardo. Atlas of the mean motion resonances in the solar system. *Icarus*, 184(1):p.29–38, 2006. doi: https://ui.adsabs.harvard.edu/link_gateway/2006Icar..184...29G/doi : 10.1016/j.icarus.2006.04.001.

- J. M. Hahn and R. Malhotra. Neptune's migration into a stirred-up kuiper belt: A detailed comparison of simulations to observations. *The Astronomical Journal*, 130(5):p.2392–2414, 2005. doi: https://ui.adsabs.harvard.edu/link_gateway/2005AJ...130.2392H/doi : 10.1086/452638.
- C. D. Murray and S. F. Dermott. *Solar System Dynamics*. Cambridge University Press, 1999.
- C. Trujillo and S. Sheppard. A sedna-like body with a perihelion of 80 astronomical units. *Nature*, 507:p.471–474, 2014. doi: https://ui.adsabs.harvard.edu/link_gateway/2014Natur.507..471T/doi : 10.1038/nature13156.
- W. Xu and D. Fabrycky. Exciting mutual inclination in planetary systems with a distant stellar companion: the case of kepler-108. *eprint arXiv*, page pp.21, 2019.
- T. Yokoyama et al. On the evection resonance and its connection to the stability of outer satellites. *Mathematical Problems in Engineering*, 2008:pp.16, 2008.